

Experimental Characterization of the Influence of Dispersant Addition on Rising Oil Droplets in Water Column

Laurent Aprin^{*a}, Frederic. Heymes^a, Pierre Lauret^a, Pierre Slangen^a,
Stephane Le Floch^b

^aLGEI, Ecole des Mines d'Alès, 6 avenue de Clavières, 30319 Ales Cedex, France

^bCedre, Centre de Documentation, de Recherche et d'Expérimentations sur les pollutions accidentelles des eaux, 715 rue Alain Colas, 29200 Brest Cedex 2, France
laurent.aprin@mines-ales.fr

The accident of the Deepwater Horizon platform in the Gulf of Mexico in April 2010 clearly shows the importance of fully understanding the oil and gas leaks phenomena in the water column and their consequences at the sea surface. While the modelling of the rise of oil droplets in the water column is widely documented, in particular through analytical model using slip velocity concept, there is a lack of information on the effect of dispersants addition on rising oil droplet. Yet dispersants, given their surfactant capacity, will necessarily modify the oil droplets behavior in the water column in terms of buoyancy due to the oil shape variations. This paper contributes to the characterization of dispersant effect on accidental oil release especially in term of physical modification for oil droplets. To investigate the study, experimental tests were performed in the Cedre Experimental Column (CEC) which is a five meter high hexagonal column with internal diameter of 1 m and total capacity of 4.50 m³ (Le Floch, 2009). This experimental device is equipped with an injection system, equipable with different nozzles diameters, and two high speed video recording systems based on shadowgraphy. It is designed to observe the shape of the droplets, including rise trail, and the dissolution rate during the ascension to the surface. This paper presents the physical modifications undergone by an oil droplet when surface active molecules are positioned at its interface with seawater. The oil droplets observation shows the addition of dispersant decreases the average droplet volume and conversely increases the number of droplets observed in the water column. Thus, the water-oil contact surface area is increased, enhancing the exchanges between these two phases, in particular in terms of the dissolution of the lightest hydrocarbon molecules. In terms of physical appearance, oil droplets showing spherical shape modify to elliptical shape from which filaments of varying sizes are fluttering. Changing shape implies a variation in the oil droplets slip velocity throughout the seawater column as well as the definition of a more complex trajectory. These two changes tend to decrease the buoyancy of oil droplets in the water column. The formation of a plume instead of surface oil slick occurs and is carried by marine currents.

1. Introduction

Since 1950, the evolutions of world demography and economic developments have led to an increase in energy requirements. Among all energies, oil remains the most needed and consumed in the world. With four billion tons in 2010, oil represents almost 33.6% of the total energetic expense. This oil demand involves risks of pollution during extraction and transport. During the last decades, many maritime accidents have occurred, resulting in major leakages of oil into the environment. Torrey Canyon accident was shipwrecked off the western coast of Cornwall, England in March 1967 and was the first large oil spill pollution in 1967. More recently, Prestige sank near the coast of Galicia through 3,500 meters deep and release 64,000 tons of crude oil. Currently, the response to these accidents consists to use dispersants in order to enhance the transfer of oil slicks from the surface to the water column, and therefore reduce the amount of oil washing up on the shore. From the other hand, for deep water oil and gas accidents the diameters of released oils droplets by

strongly influence the consequences at the sea surface. As mentioned by Brandvik, droplets larger than 5 mm rising from depth of 1,000 m could reach the water surface after many hours whereas small droplets (almost 0.5 mm) or fine droplets (below 100 μm) could last in the water for weeks or month and eventually reach the surface (Brandvik et al., 2013). Furthermore, addition of dispersant enhances oil dilution. Hence stabilization of the oil droplets in the water column increases the degradation activity by micro-organisms using carbon from the oil to grow up. Then Campo et al., 2013 analyze the biodegradability and bioavailability of dispersed oil and dispersants used for the Gulf of Mexico oil spill. They studied the biodegradation dioctyl sodium sulfosuccinate surfactant in Corexit 9500 and dispersed South Louisiana crude oil in laboratory microcosms. Prince et al., 2013 show that biodegradation of dispersed oil is prompt and extensive when oil is present at the ppm levels. Based on this argument, for the first time in the history of oil spill response, dispersants were added to oil escaping from the offshore well during the Deepwater Horizon (DWH) spill in 2010. During the DWH spill, 4,000 m^3 of dispersant were spread on the water surface, and more than 3,000 m^3 were injected at 1,500 m depth at the leak level. This response strategy immediately reduced the quantities of oil rising the surface but put in evidence questions concerning the fate of the dispersed oil in the water column. Modelling software commonly used to predict these fates provided results far from reality, due to the presence of dispersant at the oil-water interface. Therefore, it appears necessary to work on the mathematical equations describing the fate of an oil droplet within water column in order to take into account the influence of chemical dispersion (Yapa and Chen, 2004).

1.1 Theoretical aspect

In two-phase flow plumes, velocity is slipping between rising fluid particles and the surrounding liquid within the plume area. Slip velocity W_s in a droplet plume is the velocity difference between rising droplets and the surrounding liquid. The most commonly used law to calculate W_s is based on the Stokes law. The smallest single isolated droplets are approximately perfect spheres due to the dominant effect of surface tension on their shape. This law remains validate as the particles keep small, spherical, rigid and for Reynolds number smaller than unity, i.e. laminar terminal velocity. Strictly speaking this assumption is not available for larger and more turbulent particles. The velocities are then representative for small and large fluid particles where the viscosity of ambient fluid is a fundamental factor for the smallest, whereas the largest are governed by the equilibrium between the drag and buoyancy forces. Clift et al. (1978) have shown that the shape of fluid particles could be approximated by a sphere for the small size range (smaller than 1 mm), by an ellipsoid in the intermediate size range (1 mm to 15 mm), and by a spherical-cap in the larger size range. For spherical bubbles, terminal velocity is influenced by the viscosity of the ambient fluid. For ellipsoidal bubbles the interfacial tension is the key factor, while neither the viscosity of the ambient fluid nor interfacial tension influences the spherical-cap bubbles. Clift et al. (1978) offer several correlations for the different regimes of bubble shapes. Pictures presented in table 1 clearly show the regime of ellipsoidal shape is the most representative of our droplet flow. This regime is described by the following equations.

$$w_s = \frac{\mu_l}{\rho_l d_e} M^{-0.149} (J - 0.857)$$

Where

(1)

$$J = 0.94H^{0.757} \text{ for } 2 < H < 59.3$$

$$J = 3.42H^{0.441} \text{ for } H > 59.3$$

H is defined as :

$$H = \frac{4}{3} E_o M^{-0.149} \left(\frac{\mu_l}{\mu_w} \right)^{-0.14}$$

(2)

with ρ_l and μ_l respectively, the oil density and dynamic viscosity, μ_w the dynamic viscosity of water, d_e the equivalent diameter of droplet. E_o , the Eötvös number, characterizes the shape of bubbles moving in a surrounding fluid. This dimensionless parameter is proportional to buoyancy force divided by surface tension force defined as follows:

$$E_o = \frac{g(\rho_w - \rho_l)d_e^2}{\sigma}$$

(3)

σ is the interfacial tension between droplet and surrounding liquid and ρ_w the water density. M is the Morton number and as for Eötvös number, M characterizes the shape of bubbles moving in a surrounding fluid or continuous phase.

$$M = \frac{g\mu^4\Delta\rho}{\rho^2\sigma^3} \quad (4)$$

2. Experimental

The objectives of experimental investigations are the analysis and the comparison of oil and dispersed oil droplets behaviours in the water column. Experimental tests are designed to observe the shape of the droplets, their rise trail, and if possible their dissolution rate during ascension to surface.

2.1 The Cedre Experimental Column

Cedre Experimental Column (CEC) is equipped with an injection system, on which it is possible to set nozzles of different diameters. Two high speed cameras are also recording at different heights. The CEC is a five meter high hexagonal column with a diameter of 1 m and a total capacity of 4.50 m³. The experimental setup is described by Le Floch et al. (2009).

2.2 Products and Experimental Conditions

Arabian light crude oil is used to characterise droplets behaviour, as the oil viscosity needs to be low, otherwise the injected oil forms filaments instead of droplets. Moreover Arabian oil viscosity is about 10.2 cSt at 15 °C. The oil density is 0.844. The dispersed oil is a mix of Arabian oil and 5 % volume of dispersant (Corexit 9500). Injection is performed at 4 m depth at the column centre with an injection nozzle of 1.5 mm in diameter. The injection flow rate is provided by a pump at about of 30 mL/min at atmospheric pressure. It is noticed for this flow rate droplets are close together and may interact. The outlet pressure is low in order to avoid jet dynamics.

2.3 High Speed Imaging by Shadowgraphy

The experiments performed in the CEC are recorded in shadowgraphy. This optical technique was developed by Settles (2001) to visualize the optical inhomogeneities in transparent media. This technique was used in previous works by Slangen et al., (2010) and Aprin et al. (2014) to analyse the chemicals solubilization mechanisms in seawater. The first camera (CAM0) is located 15 cm above the injection nozzle (4 m depth), and the second (CAM1), 15 cm below the surface (0.15 m depth). Cameras frame rate is 64 frame.s⁻¹ with a resolution of 640 x 840 pixels. The area of interest represented 3.42 x 2.57 cm, for CAM0 and 2.46 x 1.85 cm for CAM1 corresponding respectively to a pixel resolution of 53.5 µm and 38.5 µm. Each sequence of image was processed to locate and track the droplets. This tracking algorithm based on the detection of differences of grey levels for each pixel on the image, detects the droplets (dark) from the background (bright). The uncertainties on droplet diameter are about 20 pixels which represents between 5 % to 20 % of diameter depending on the droplets diameters. The droplet velocity is obtained through the calculation of the distance travelled by the droplet between two images (interframe time is 15.6 ms). The equivalent diameter is calculated by the Waddel disk diameter which is defined as the diameter of the disk with the same area as the particle (Fuhrer et al., 2011). The Heywood circularity factor is calculated to describe the shape of the particle, the closer the shape of the particle is to a disk, the closer this factor is nearby 1. It corresponds to the ratio of a particle perimeter to the perimeter of the circle with the same area.

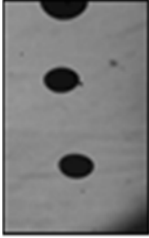

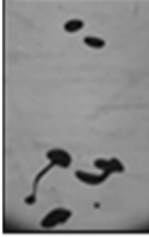

3. Results

3.1 Particle Shape without and with Dispersant

For the same injection conditions, the shape, and consequently the behavior, of oil droplets and dispersed oil droplets were very different. Table 1 presents images of the droplets at 4 m depth and 0.15 m depth. Pure oil provided spherical-shaped particles at both depths. The Heywood Circularity Factor (HCF) confirms the homogeneity of the oil droplets population, which were spherical for sizes lower than 6.3 mm. Oil with added dispersant produces filament-shaped, ellipsoidal and a few spherical-shaped particles. With dispersant (oil + 5 % vol. dispersant) the HCF confirms droplets have various types of shapes and are highly different at 4 m depth and 0.15 m depth. In this condition, the effect of dispersant is clearly observed: with dispersant the oil droplets' shape changed during their ascension in the water column. The droplets are flatter and lose an

important amount of matter, forming filaments and smaller droplets, due to physical erosion processes linked to the friction force and solubilization processes.

Table 1: Shape of oil droplet and dispersed oil droplet observed at 4 m depth and 0.15 m depth.

	4 m depth	0.15 m depth
Oil	<p>Spherical shape</p>  <p>Heywood circularity factor mean: 1.05 ± 0.05 minimum value: 0.83 maximum value: 1.43</p>	<p>Spherical shape</p>  <p>Heywood circularity factor mean: 1.01 ± 0.04 minimum value: 0.84 maximum value: 1.34</p>
Oil + Dispersant	<p>Spherical, ellipsoidal and filaments shaped</p>  <p>Heywood circularity factor mean: 1.14 ± 0.05 minimum value: 0.75 maximum value: 3.45</p>	<p>Spherical, ellipsoidal and "jellyfish" shaped</p>  <p>Heywood circularity factor mean: 1.11 ± 0.26 minimum value: 0.76 maximum value: 2.513</p>

3.2 Particle Distribution with and without Dispersant

The sizes of the droplets were compared in both conditions, with and without dispersant, for both levels (0.15 m and 4m depth). For oil without dispersant, three different populations of droplets are observed; one with an equivalent diameter between 0.2 mm and 0.8 mm, mainly represented at 4 m depth with a frequency of 60 % of the droplets, the other between 3 mm and 3.7 mm (8 % at 4 m depth and 17.5 % at 0.15 m depth) and the last group mainly represented at 0.15 m, with a frequency of 60%, between 0.3 mm and 5.4 mm (Figure 1a). In the case of dispersed oil, at 4 m depth most of the droplets are smaller than 1 mm (over 37 % of the total population) and larger droplets appear between 1 mm and 6 mm. At 0.15 m more than 88 % of the droplets are ranged between 0 and 1 mm (Figure 1b). These results clearly show the oil droplets without dispersant coalesce during their ascension in the water column (higher percentage of small particles at 4 m than at 0.15 m). When dispersant is added, the larger droplets are fragmented during their rise to the surface (percentage of small droplets increase from 37 % at 4m depth to 88 % at 0.15m depth).

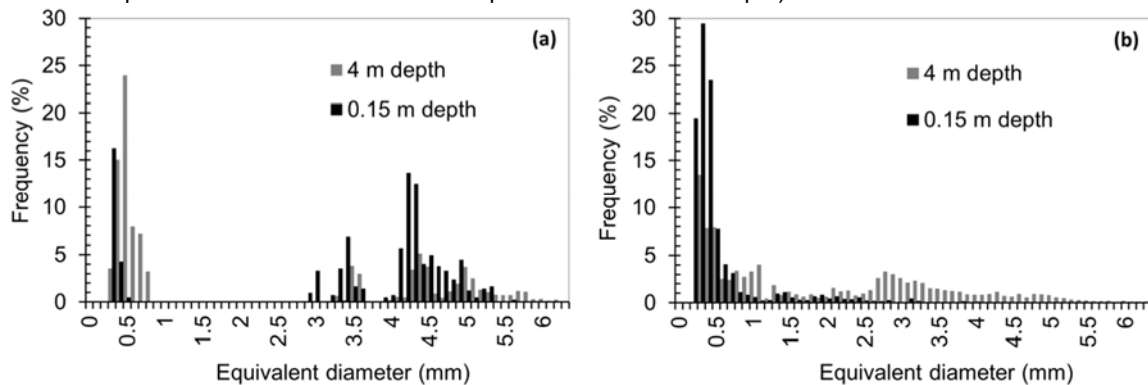


Figure 1: Particle distribution at 4 m depth and 0.15 m depth for a) oil, b) dispersed oil (oil + 5% of dispersant)

3.3 Characterization of oil droplets velocity in the water column with and without dispersant

As explained in section 1.1, droplets velocities are influenced by the size of the particle as shown by the nonlinear Clift's formulation (Li and Yapa, 2000). Figure 2 and Figure 3 present the droplet rising velocities as a function of droplet diameter for oil and oil + dispersant experiments, respectively. The model proposed by

Clift to evaluate the terminal velocity for droplet (Eq.1) is also plotted on Figure 2 and Figure 3. The comparison between the two figures clearly shows differences: the nonlinear relationship with the droplet size, and the difference for velocities at same droplet size between oil and oil + dispersant experiments. This remark is mainly due to the droplet shape difference. Oil + dispersant droplets are flattened and present ligaments in the droplet wake which causes higher friction effects, interactions between droplets and induces lower velocities. It is noticed on Figure 2 two different groups of data which seems to follow a different equation from the second group of data. This difference can also be attributed to the different shapes characterizing these droplets. When the droplets are smaller than 1 mm their shape is spherical, whereas the larger droplets are more elliptical shaped. Nevertheless, the terminal velocity limit seems to be lower when dispersant is added (<0.15 m/s). The consideration, which needs to be statistically strengthened with additional data, is that the addition of dispersant seems to decrease the rise velocity of the droplets. In addition, the comparison between experimental data and Clift's correlation for the Figure 2 and Figure 3 shows discrepancies due to measurements uncertainties (about 10 % on droplet diameter) and the droplet oscillations. The oil droplets without dispersant follow the Clift's curve plotted with an interfacial tension value of 0.032 N/m. However, the oil droplets with dispersant follow the Clift's curve plotted with an interfacial tension value of 0.00086 N/m. This result indicates that the addition of dispersant greatly decreases the interfacial tension of the oil droplets. And a decrease in this interfacial tension results in a decrease in the rise velocity of the oil droplets.

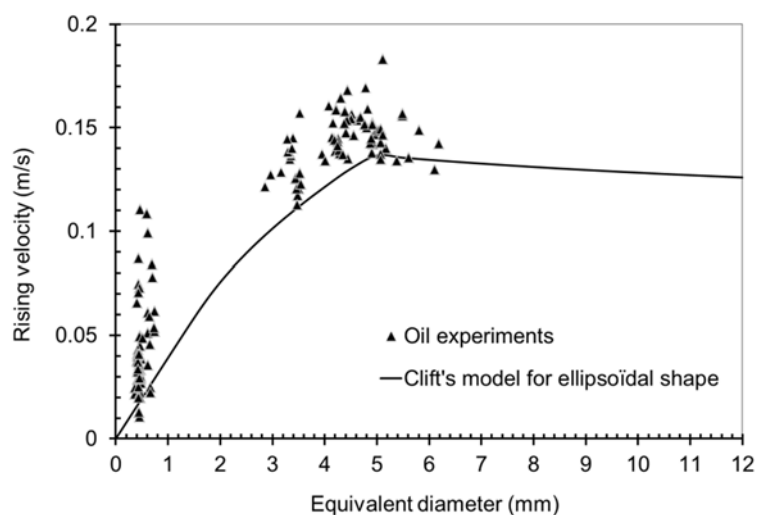


Figure 2: Rising velocity for oil droplets experiments vs equivalent diameter. Comparison with Clift model for ellipsoidal droplet shape

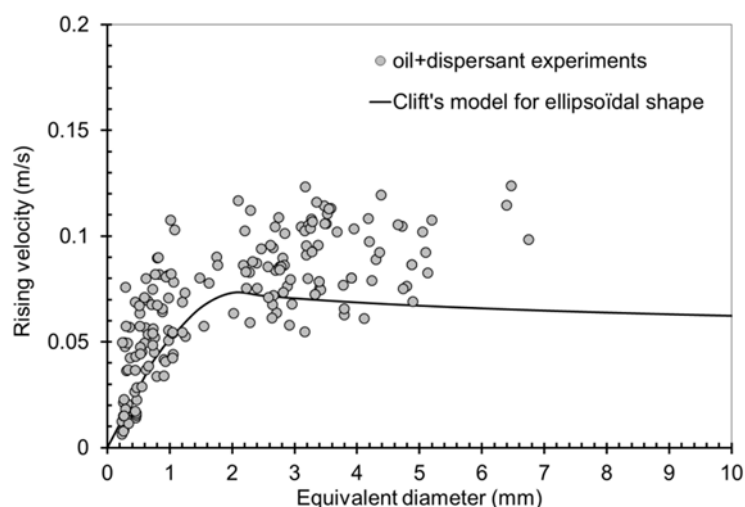


Figure 3: Rising velocity for oil + dispersant droplets experiments vs equivalent diameter. Comparison with Clift model for ellipsoidal droplet shape

4. Conclusion

This work presents promising experimental results regarding the behaviour differences between oil droplets and oil with added dispersant (Corexit 9500) in the water column in terms of velocity, shapes and diameter distribution. Ongoing experimentation, using the same approach, will increase the number of samples and strengthen the confidence in these results from a statistical point of view.

However, as a preliminary conclusion, it has been clearly demonstrated that dispersant addition reduces the size of oil droplets and changes their shape, and in doing so alters their rise velocity within the seawater column. Dispersant ability to reduce the surface tension of oil droplets is underlined; it also appears to prevent the coalescence of droplets and increases their dissolution.

Currently, Clift's equations appear to be the most suitable although questions remain over the interfacial tension values to be used. Additional physico-chemical phenomena emphasized in this paper should be implemented in software models designed to forecast the fate of a subsea oil leak. Finally, this work deserves to be supplemented by experiments with other crude oils with various physical properties designed to characterise the fate of oil droplets for various injection rates and also by varying the pressure within the water column.

References

- Aprin L., Heymes F., Fuhrer M., Slangen P., Dusserre G., Le Floch S., 2014, Experimental analysis of n-butanol behavior in seawater due to chemical release from marine shipwreck, *Chemical Engineering Transactions*, 36, 19-24, DOI: 10.3303/CET1436004.
- Brandvik J., Johansen O., Leirvik F., Farroq U., Daling P.S., 2013, Droplet breakup in subsurface oil release – Part 1: Experimental study of droplet breakup and effectiveness of dispersant injection, *Marine Pollution Bulletin*, 73, 319-326, DOI: 10.1016/j.marpolbul.2013.04.012.
- Campo P., Venosa A.D., Suidan M.T., 2013, Biodegradability of Corexit 9500 and Dispersed South Louisiana Crude Oil at 5 and 25 degrees C, *Environmental Science & Technology*, 47, 1960-1967.
- Clift, R., Grace J.R., Weber M.E., 1978, *Bubbles, Drops and Particles*, Academic Press, New York.
- Fuhrer M., Slangen P., Aprin L., Dusserre G., Le Floch S., 2011, A New Approach to Analyze Chemical Releases Behavior in Water Column: High Speed Imaging, *Proceedings of 2011 International Oil Spill Conference (IOSC)*, Portland, Oregon, USA.
- Le Floch, S., Benbouzid H., 2009, Operational Device and Procedure to Test Initial Dissolution Rate of Chemicals after Ship Accidents: The Cedre Experimental Column, *The open Environmental Pollution & Toxicology Journal* 1, 1-10.
- Li, Z., Yapa P.D., 2000, Buoyant Velocity of Spherical and Non-spherical Bubbles/Droplets, *Journal of Hydraulic Engineering*, Members ASCE, 126, 852-854.
- Prince R.C., McFarlin K.M., Butler J.D., Febbo E.J., Wang F.C.Y., Nedwed T.J., 2013, The primary biodegradation of dispersed crude oil in the sea, *Chemosphere*, 90, 521-526.
- Settles G.S., 2001, *Schlieren and Shadowgraph Techniques: Visualizing Phenomena in Transparent Media*, Springer Verlag.
- Slangen, P., Aprin L., Fuhrer M., Le Floch S., Dusserre G., 2010, Methyl Ethyl Ketone Spills in Water: Visualisation of the Releases by Optical Schlieren Technique, *Proceedings of 33th AMOP Technical Seminar on Environmental Contamination and Response*, Environment Canada, Ottawa, Ontario, Canada.
- Yapa, P.D., Chen F., 2004, Behavior of Oil and Gas from Deepwater Blowout, *Journal of Hydraulic Engineering*, 130, 540-553.